Journal of Energetic Materials
Publication details, including instructions for authors and subscription information:
http://www.informaworld.com/smpp/title~content=t713770432

Real-time analysis of the reaction products of shocked solid nitric oxide

Normand C. Blais[a]; N. Roy Greiner[a]
[a] Division Los Alamos National Laboratory, Chemistry and Laser Sciences, Los Alamos, NM

To cite this Article Blais, Normand C. and Greiner, N. Roy(1988) 'Real-time analysis of the reaction products of shocked solid nitric oxide', Journal of Energetic Materials, 6: 3, 255 — 281
To link to this Article: DOI: 10.1080/07370658808012556
URL: http://dx.doi.org/10.1080/07370658808012556

Real-Time Analysis of the Reaction Products of Shocked Solid Nitric Oxide

Normand C. Blais
N. Roy Greiner
Chemistry and Laser Sciences Division
Los Alamos National Laboratory
Los Alamos, NM 87545

We have determined the reaction products from shocking solid NO. The shock was sufficient to produce detonation products. Small charges of NO at a temperature of 30 K are shocked by detonating PETN boosters in a high vacuum apparatus. The expanded products are allowed to form a molecular beam and are detected by a mass filter as a function of time after detonation. The principal products are N_2, O_2, N_2O, and NO_2. We can account for the product intensities on the basis of a simple mechanism:

$$NO \rightarrow 1/2\ N_2 + 1/2\ O_2 \qquad (1)$$

$$NO + 1/2\ O_2 \rightarrow NO_2 \qquad (2)$$

$$NO \rightarrow 1/3\ N_2O + 1/2\ NO_2\ . \qquad (3)$$

Each reaction consumes 19%, 10%, and 36% respectively of the NO in the charge. The threshold velocity of 7 km s^{-1} for N_2 and O_2 indicate that detonation of NO contributed to these products. We present the results of a Langrangian computer model of the free expansion to interpret the dynamics and the chemistry in our experiments. It confirms that reactions are rapidly quenched by adiabatic cooling and that the product flow becomes self-similar after expansion of only a few charge diameters.

Journal of Energetic Materials vol. 6, 255-281 (1988)

Published in 1988 by Dowden, Brodman & Devine, Inc.

We've also obtained an absorption spectrum of one of the products, NO_2, in the wavelength region 430–472 nm. The internal temperature of these molecules is about 300 K, much lower than the estimated detonation temperature of 2500 K.

INTRODUCTION

The explosive propensities of condensed phase nitric oxide are well known.[1-3] The sensitivity of liquid NO to shock-initiated detonation is somewhere between that of nitroglycerine and nitromethane. A shock pressure of 10 GPa develops in the liquid during detonation, and the temperature is estimated to reach 2500-3000 K at a density of about 2 g/cm^3. The velocity of the detonation wave is 5.6 kms^{-1}. Because of its simple chemical constituency, it is a very attractive substance to consider as a model explosive. It is being studied extensively at this laboratory, one of the intended goals being to reveal the important chemical reaction mechanisms that provide the driving energy of the detonation.

Accurate detonation velocity measurements by Davis[3] and the determination of the equation of state of the post shock products by Schott,[4] combined with theoretical models, indicated that the products were principally N_2 and O_2 with some oxides of nitrogen. However, no independent or direct determination of the detonation products was available. We report here the real-time measurement of the mass spectrum of highly shocked, partially detonating solid nitric oxide. It confirms that N_2 and O_2 are important products of detonation, so that the overall reaction

$$NO \rightarrow 1/2\ N_2 + 1/2\ O_2 \qquad (1)$$

is a significant source of energy to drive the detonation.

We also report the absorption spectrum of the detonation products at 430 to 471 nm and discuss its characteristic with respect to a computational model of our laboratory scale detonations.

EXPERIMENTAL

For our apparatus to function as intended, no collisions must occur between the product molecules and ambient molecules before they are detected. The gases at the leading edge of the expanding volume of detonating products must have a mean free path of a meter or more before they are formed into a molecular beam, after which even inter-product collisions are infrequent. We try to maintain an apparatus pressure of 1 mPa (10^{-5} torr) before detonation. Nitric oxide boils at –151°C and remains a liquid over a 10°C range to -161°C. Therefore the ambient pressure requirement means that we are constrained to work with NO initially in its solid phase. Consequently the structure which supports the NO charge and its detonator is capable of operating at cryogenic temperatures

Aside from the cryogenic requirements, the apparatus we used was one that we described earlier[5] in connection with studies of solid explosives. An important modification was made to the carousel containing the detonator stations so that it could be cooled to low temperatures while still serving the function of aligning sequentially several NO charges with the detector axis. Our carousel was thermally isolated as much as feasible from the rotary table which served to align the charges. For low temperature use we found it necessary to reduce the size of the original carousel, which could accommodate 30 explosive charges, to 6 charges. Cooling was accomplished by connecting a dozen strands of flexible copper braid between the second, low temperature, stage of a stationary He cryocooler and the top of the carousel.[6] The principal source of heat was radiation and conduction along the low inductance firing cables that initiated the detonation. Figure 1 is a sketch of the apparatus and shows the essential features of the experimental arrangement.

Not shown in the figure, for the sake of clarity, is an aluminum shroud that surrounded the carousel and served as a radiation shield. It was attached to the first stage of the He cryocooler which maintained it

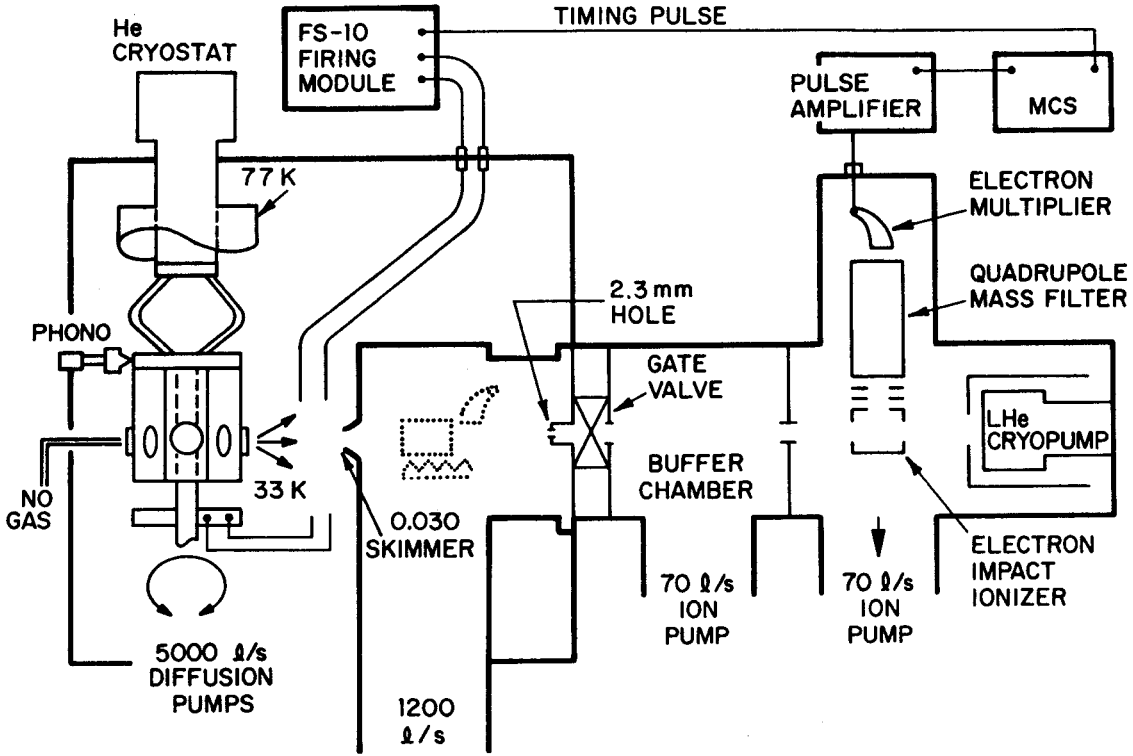

FIGURE 1

A schematic drawing of the apparatus. The distance from the detonation point to the electron impact ionizer is 122 cm, from the detonation point to the skimmer it is 53 cm. The dotted apparatus behind the skimmer represents an alternative location for a detector or an auxiliary experiment to check time-of-flight measurements. The phono needle is an ordinary crystal phonograph pickup to measure the impulse delivered to the detonator station upon detonation.

NORMAND C. BLAIS
ROY GREINER

nominally at 77 K. There were two holes in the shroud, one being centered on the detector axis. When an NO charge was centered for detonation it was also opposite the hole, so that the expanding gaseous products were unimpeded by the shroud, especially those that traveled along the detector axis. The other hole allowed access to each cold detonator station with a gas jet by which NO gas was condensed over the center of the detonator.

The jet was a multichannel capillary array[7] on the end of an externally manipulated tube. Generally the end of the capillary was about 1 mm from the layer onto which NO was being deposited. At steady-state conditions, the temperature of the carousel was usually between 30-35 K. With a pressure of 20 torr behind the jet, we measured a flow rate of 3×10^{-5} mol/sec, and we detected only a 0.1 mPa pressure rise in the apparatus indicating an efficient condensation on each station. From other experiments we did with a similar detonator arrangement, we estimate that 80% of the gas effusing from the capillary sticks to the detonator. The usual charge consisted of 25–35 mmol of condensed NO.

Figure 2 is a sketch of a detonator station arrangement. The design shown has two essential features. One is a PETN/electrical slapper that serves to shock the NO to detonation. The PETN is in a 25-mg pellet with 1.50-1.60 g/cm^3 density. The slapper is a 0.05-mm-thick Kapton plastic onto which a copper bridge is vapor deposited. An electrical pulse with 2.5 J delivered in less than 10 ns to this bridge starts the process. The other feature is an arrangement to ensure a cold surface upon which to deposit the NO gas to a solid. A 0.025-mm aluminum foil covers the PETN pellet and is clamped to make good contact at the cooled carousel. This foil is a reasonably good density match with the pellet through which the shock can pass to the NO. For some tests, we tried partial confinement of the deposited NO by replacing the top steel plate clamping the Al foil to the carousel structure with a 3-mm-thick copper plate with a 7.5–mm hole. The NO gas was deposited into the cup formed by the copper plate and the Al foil as the bottom. With this latter arrangement we could even tamp the depositing NO with the flat tip of the capillary

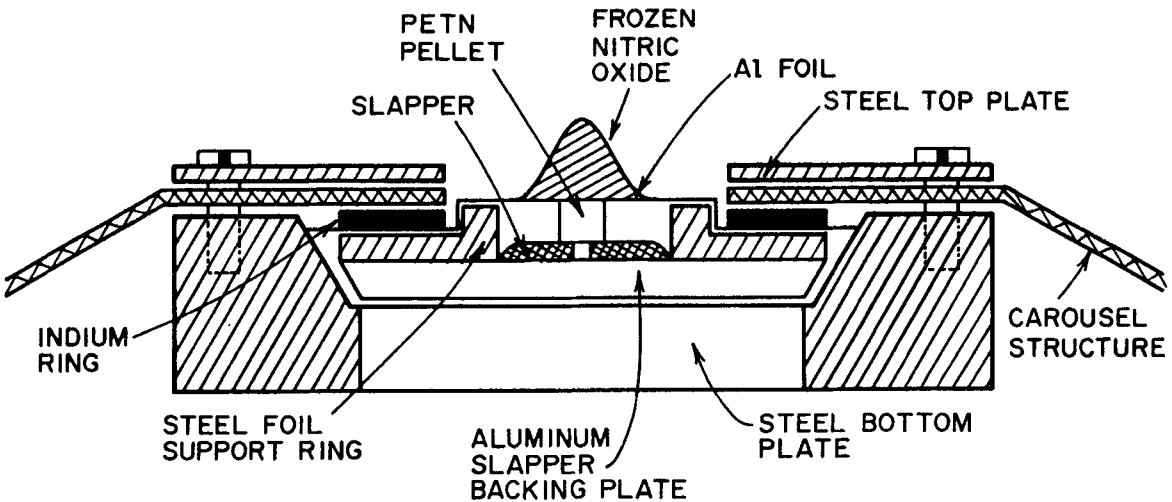

FIGURE 2

A cut–away sketch of one of the cryocooled detonator stations. The slapper is 0.01-in.-thick Kapton upon which a thin copper bridge has been deposited. The entire assembly is maintained at 30 K.

NORMAND C. BLAIS
ROY GREINER

array, much like packing a snowball, to increase its density. We were hoping to increase the fraction of NO used up in the detonation over that using the unconfined geometry. Of course, the hot capillary tip evaporated some of the deposited NO during tamping, but we were able to judge the amount of NO being used by always filling the confining cup, although we were uncertain about the final density.

The velocity of the various molecular products was measured the same way as was reported earlier,[5] using time-of-flight methods. For these experiments, the flight distance was slightly longer, 1.22 m. The typical flight times were then somewhat longer than we reported then. However, we want to emphasize that although our measuring times are long compared to the detonation events we are examining, they do not affect the time scale over which products can be changed by reaction after detonation. If we doubled or halved the observation times (by changing the detector-to-detonation distance) our mass spectrum would be the same. What determines how representative our product spectrum is of any particular region in which it was produced, in or after the reaction zone, is the number of collisions these molecules have with other molecules before they are detected. Under our conditions this is determined by the adiabatic expansion into the vacuum. Those products that were formed near the surface of the charge toward the detector expand the most rapidly until the temperature is low enough that product states are "frozen." Model computations, some of which we describe later, indicate that the time it takes for this to occur after detonation is about 1 to 2 μs. This is the "real time" over which we do our analysis. This is still long compared to the time for passage of a detonation wave through our charges, but we feel that possibly we can observe some of the species that are present in the reaction zone of a detonation.

Another view of the reaction chamber is shown in Fig. 3, which we provide principally to describe how we obtain the absorption spectrum. Two 45° aluminum mirrors deflect the light collected from a point source Xe flashlamp (ILC model L1821 operated at 3.0 KV with a 0.2 μF capacitor)

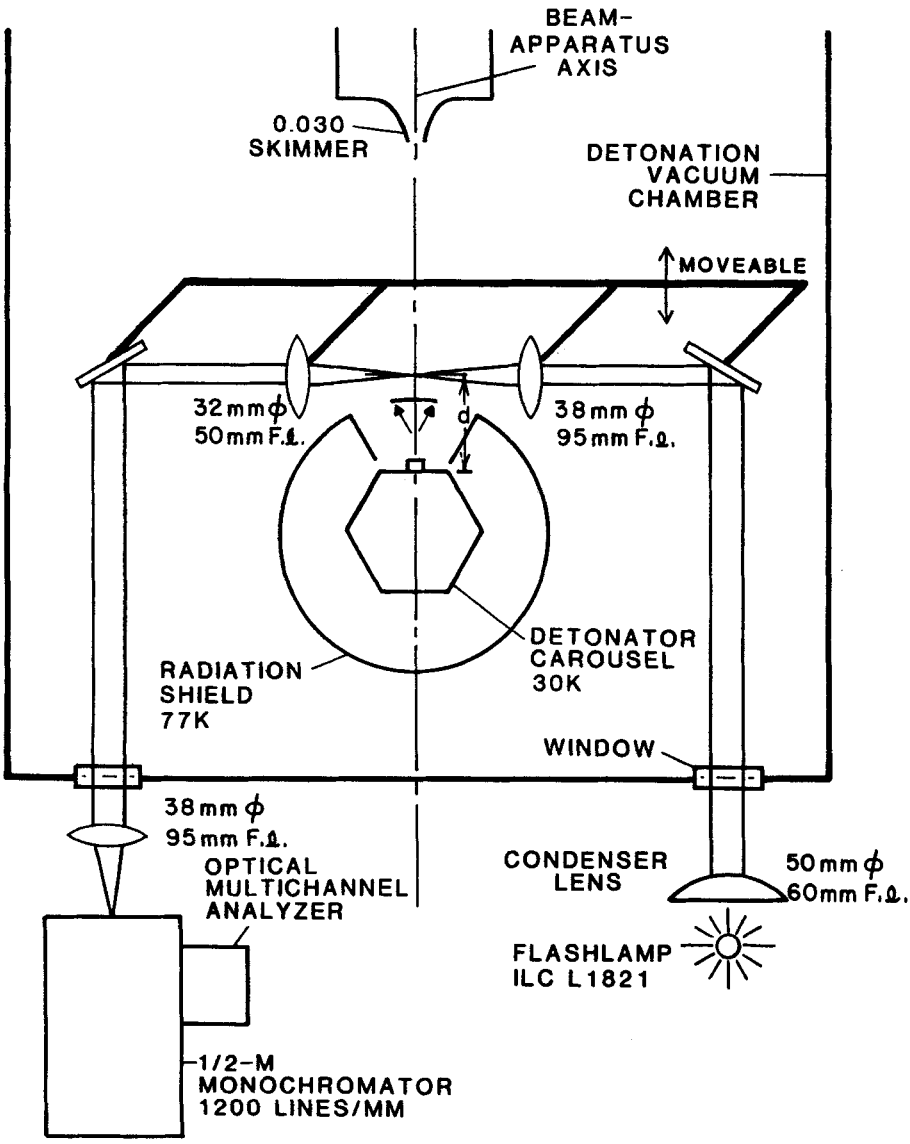

NORMAND C. BLAIS
ROY GREINER

FIGURE 3

A top view of the detonation chamber of Fig. 1 showing the mirror arrangement used to obtain the absorption spectrum of Fig. 5. The mirror and lens structure is moved in the vacuum system by a small motor and screw arrangement to locate the focused light at various distances along the axis of the expanding detonation products.

and steer it across the path of the expanding gas products. This lamp produces a continuous spectrum from 400 nm to 550 nm.

Two lenses mounted between the mirrors focus it to a cross section about 5 mm diameter at the apparatus axis. A 1/2-m monochromator (Jarrel-Ash 82-546, with 1200 lines/mm grating) dispersed the transmitted light and refocused it into an intensified optical multichannel analyzer (OMA, Tracor Northern TN6100). The optical system was triggered with variable delay after the detonating current was delivered. The light pulse from the flashlamp was less than 1 μs long at 10% above baseline. The structure supporting the 45° mirrors and focusing lenses was movable along the apparatus axis so that the distance from the NO charge-to-the-light focus could be changed from one shot to another.

RESULTS

Mass Spectrum

The mass spectrometer data of the reaction products are shown in Fig. 4. They show the counts collected in each channel of the multichannel scaler. The abscissa has been labeled in time using $t = (n-1/2)\Delta t$, where n is the channel number and Δt is the dwell time per channel. The MCS sweep is triggered by the detonating current and Δt is normally 10 μs.

These are the principal ion signals that we detected, although we looked at other mass settings of the detector, including, M = 14, 60, 62, and 76. Both the time dependence of the M=16 signal and the known electron impact fragmentation characteristics of NO_2[8] suggest that M=16 is not a detonation product but that it is produced in the mass spectrometer ionizer. The M=30 signal is unused NO that is heated by the reactions in the NO and by the PETN booster. Masses 28 (N_2), 32 (O_2), 44 (N_2O) and 46 (NO_2) are the principal reaction products. We detected no significant amounts of nitric oxide dimers NO_3 or N_2O_3. Other masses heavier than M=46 were absent, so that we feel confident that these four species are produced in the reacting NO and are not, like M=16, cracking fragments produced in the detector.

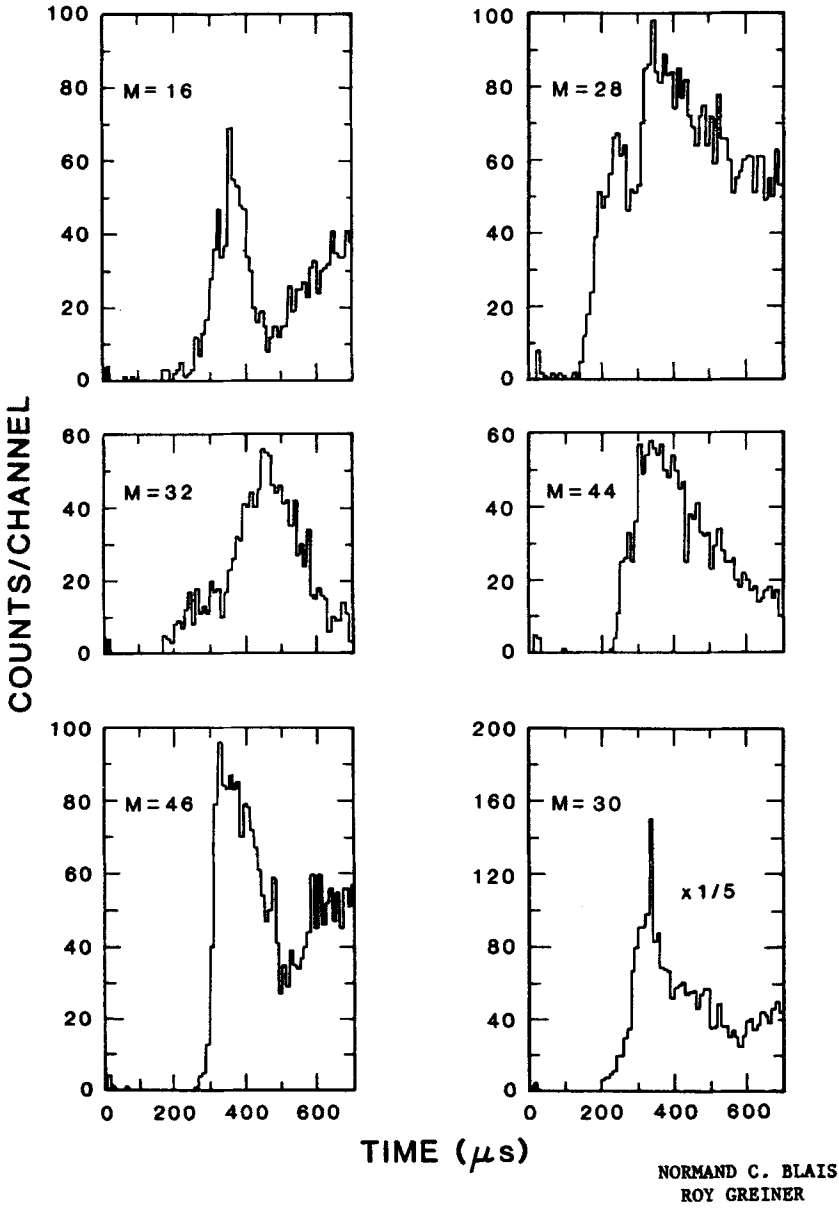

FIGURE 4

Histograms of the raw data for the various products as observed on the multichannel scaler. The horizontal axis has been converted from channel number to a time scale. All scaler dwell times were 10 μs/ channel.

Of the four principal products, the threshold of product arrival at the detector is earlier for N_2 and O_2 than it is for N_2O and NO_2. This is unlike the results obtained for more common explosives,[5,9] where it is found that almost all products have the same threshold of arrival, irrespective of mass. There are several possible explanations for this difference. One possibility is that the product expansion for nitric oxide although homogeneous, is much different than for other explosives, being less strongly driven. That is, the velocity imparted by the expansion process is not much larger than the mean velocity of the newly formed products before expansion. This possibility does not seem very likely, since the velocity of the N_2 and O_2 products in this threshold region is 7 kms^{-1}, nearly the same as product velocities we obtain for HNS or PETN. Another, and more likely, possibility is that N_2O and NO_2 are formed at later times, when the product expansion is already progressed. They are formed deeper in the product cloud and therefore arrive later than N_2 and O_2. We found a similar behavior in the clusters of carbon formed in HNS detonations.[9] They too arrived anomolously late, but with increasing cluster size.

Velocities of the magnitude we measure for N_2 and O_2 identify these products as detonation products. Our experience with other substances, explosives and inert substances, indicate that we do not attain molecular speeds this high without detonation. These then we call direct detonation products, which probably are formed in the reaction zone following the pressure front. As we will discuss shortly, some of the NO_2 product comes about because of the presence of O_2 product and unused NO, so that it is formed at a later time, in which case we characterize it as a secondary product (although not necessarily all of it). Because not all of the NO is consumed in the reactions, we cannot state the time sequence of the product formation. The poorly controlled condition of the initial NO charge, principally the density and size, would have probably made it impossible to make a measurement of the reaction zone size, or to identify a CJ point if it existed here. We attempted some experiments in which thin layers of isotopically labelled $^{15}N^{18}O$ were deposited at

various stages of the charge buildup to see if we could identify the time-of-arrival of these layers at the mass spectrometer detector. This would have established a time scale correspondence of the time-of-flight data with the product expansion process. Unfortunately, the results were inconclusive for reasons we have not yet determined.

To obtain a quantitative measure of the product spectrum, we transformed the data of Fig. 4 from number density distributions to flux distributions.[10] The integral of the flux intensity is the amount of product of each mass produced. We limited the integration to 620 μs to be certain that only direct products were being considered. Adjustments to the flux were made to account for the measured relative mass transmission of the detector and the ionization efficiency of each species relative to N_2.[11] Table I is a summary of the average of data from several shots, each with the mass spectrometer set at the indicated mass. On each data histogram, of the kind shown in Fig. 4, we draw a curve passing as closely as

TABLE 1.

A summary of mass spectrum of solid nitric oxide reactions: the intensity at each mass, the instrumental adjustments, the integrated flux.

Product Molecule	Mass	Total Counts[a]	Adjustment	Normalized Integrated Flux[b]
O atom	16	936	----	
N_2	28	2644	1.00	2644
NO	30	10230	0.87	9944
O_2	32	840	1.35	1254
N_2O	44	1328	0.88	1279
NO_2	46	1860	2.50	4278
$(NO)_2$	60	0	---	0
NO_3	62	0	---	0
N_2O_3	76	0	---	0

[a]Sum of counts in each multichannel scaler channel up to channel at 620 μs.

[b]Adjusted by factors in previous column, integrated to 620 μs.

possible through the points within the statistical error associated with that point. The curve was represented analytically using a cubic spline and the transformation to flux was done numerically as well as the integration of the flux. The column labeled "adjustment" was the multiplicative factor that adjusts for the mass and ionization sensitivity.

We can account for the final mass spectrum resulting from highly shocked NO on the basis of three reactions: Eq. (1) and Eqs. (2) and (3) below. Reaction 2 is a well-known reaction in the gas phase.[12] Reaction 3 is intended to represent an overall reaction involving only nitric oxide that forms NO_2 and N_2O, and in a detailed kinetics scheme may be much more complex than as written here.

$$NO + 1/2\ O_2 \rightarrow NO_2 \qquad (2)$$

$$NO \rightarrow 1/3\ N_2O + 1/3\ NO_2\ . \qquad (3)$$

A material balance based on the three reactions leads to Eq. (4), which shows how the integrated fluxes of Table I should be related. Our data satisfies the equation to within a few percent.

$$N_2O + 2N_2 = 2O_2 + NO_2\ . \qquad (4)$$

In Table II we have listed reactions 1, 2, and 3, the relevant heats of reaction for each, and the fraction of the nitric oxide that was consumed

TABLE 2

Reactions leading to observed products, their heats of reaction and the fraction of nitric oxide consumed in each reaction.

Reaction	ΔH, kcal/mole	Fraction NO Consumed
(1) $NO \rightarrow 1/2\ N_2 + 1/2\ O_2$	-21.6	0.19
(2) $NO + 1/2\ O_2 \rightarrow NO_2$	-13.7	0.10
(3) $NO \rightarrow 1/3\ N_2O + 1/3\ NO_2$	-12.4	0.36
Total		0.65

in each. Both Tables I and II came from analysis of runs in which the solid NO was contained and packed (as described in the Experimental section). Shots for which the NO was deposited on the aluminum foil only and not packed gave very similar results to those shown in the tables. Thus the packing may have increased the net amount of NO consumed, but the spectrum and the fractional usage by each reaction was comparatively unchanged.

Absorption Spectrum

Figure 5a shows the absorption spectrum taken when the light from the flashlamp was focused on the instrument axis at a distance of 4.0 cm from the NO deposit. The flash was delayed by 25 μs. For comparison in Fig. 5b, we show the absorption in a quartz cell of NO_2 at a partial pressure of 500 Pa and a temperature of 22°C. It is clear by comparing Figs. 5a and 5b that the absorbing material in the products is NO_2. Figure 5c shows the change in the spectrum with the gas temperature, upon raising the temperature to 200°C. For these comparisons, most of the gas in the cell was O_2 at a pressure of 4.5 kPa so that NO_2 dissociation was less than 3%, assuring us that the spectrum changed because of hot bands and not because of gas composition changes.

The average molecular temperature of the product NO_2 is clearly room temperature or lower. It is the sharpness of the molecular band structure and the number of such sharp features that can be distinguished that must be compared between the three top panels of Fig. 5 to estimate the temperature of panel (a) and not necessarily the intensities of the absorption bands. Several small features are visibly "washed out" of panel (c) as compared to either panel (a) or panel (b). These absorbing molecules had a velocity of 1.6 kms^{-1}, about one-half the speed of highest intensity product NO_2 of Fig. 4. No absorption was evident when the light flash delay was reduced to 13 μs, even though the mass spectrometer showed the usual intensity and time of arrival of NO_2. Thus it seems that the molecules responsible for the strong absorption are not representative of those giving the strongest ion intensity in the mass spectrometer detector.

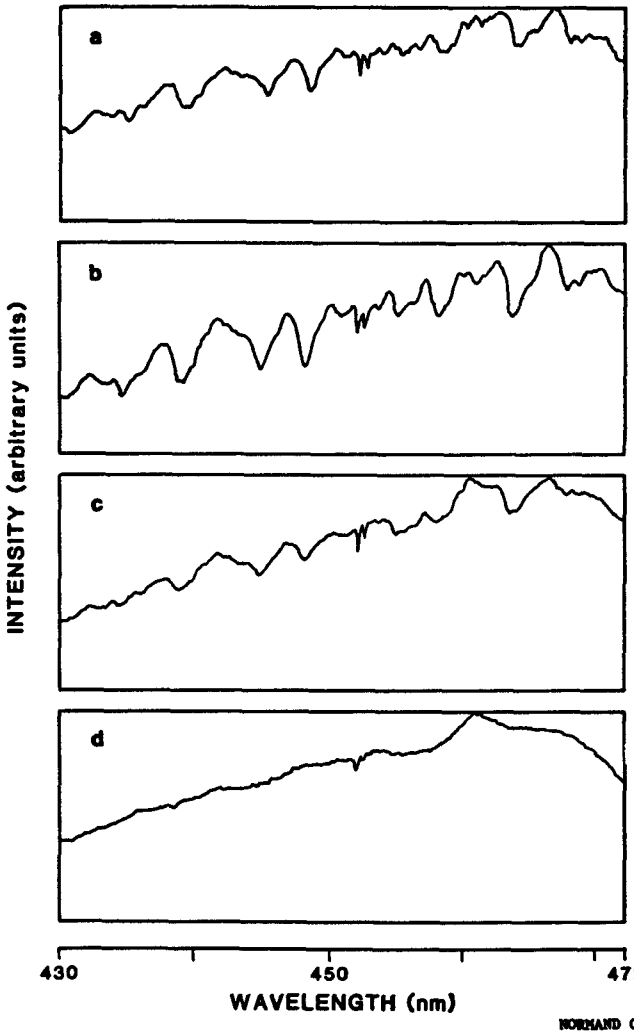

NORMAND C. BLAIS
ROY GREINER

FIGURE 5

The spectrum of the transmitted light using the arrangement of Fig. 3. Panel (a) was obtained when the only absorbers were the detonation products. The light was flashed 25 μs after detonation and was focused 4.0 cm from the detonation point. Panel (b) is the spectrum obtained when a cell containing 500 Pa of NO and 4.5 kPa of O_2 was put between the lenses of Fig. 3. The cell was 9.5-cm long and at a temperature of 22°C. Panel (c) is when the cell was at 200°C. Panel (d) is a blank firing to show the lamp spectrum.

HYDRODYNAMIC MODELING AND THE OBSERVED SPECTRA

The hydrodynamics of the flow of the NO reaction products were modeled with an adaptation of the Los Alamos reactive hydrodynamics code KIVA.[13] KIVA can model fluid dynamics with ongoing chemical reactions, and is particularly useful for modeling free expansion of a dense fluid, such as explosive products, into a high vacuum. For the purposes of modeling these experiments, we used a P-V equation of state that matches faithfully the BKW expansion isentrope[14] of PETN from the Chapman-Jouguet (CJ) point[15] down to about 1 kbar.[16] Below 1 kbar it asymptotically approaches an ideal gas isentrope. The initial density was adjusted so that an isentrope of this form gave a computed time-of-arrival (Fig. 6) that matched the observed one (Fig. 4). It was then used to model the hydrodynamics (mass flow and densities) of the product plume as it expands into the vacuum. Velocity fields (Fig. 7) and density profiles (Figs. 8 and 9) were calculated as a function of time. With the initial conditions of these experiments the flow becomes self-similar after 7 μs. This means that the plume grows in size at a constant rate, the velocity of each mass element remains constant (Fig. 7), and the spatial distribution of mass in the plume remains invariant with time (Fig. 8) as long as the plume expands freely and does not collide with anything. This model of the plume hydrodynamics allows us to map information from the observed time of arrival of species at the mass spectrometer back to positions in the plume (along the z-axis) at any time during the expansion. In this study it was assumed that the relative product concentrations remain invariant during the observation times, i.e. from 13 μs after the detonation of the booster until the end of the product arrival-time trace.

The temperatures were calculated from the densities using a crude power-law expression that matched the BKW results in the CJ region and paralleled the ideal gas values at densities below 0.1 g/cm^3. The temperatures given by this expression in the ideal gas region may be somewhat low, depending on the actual molecular weight of the product

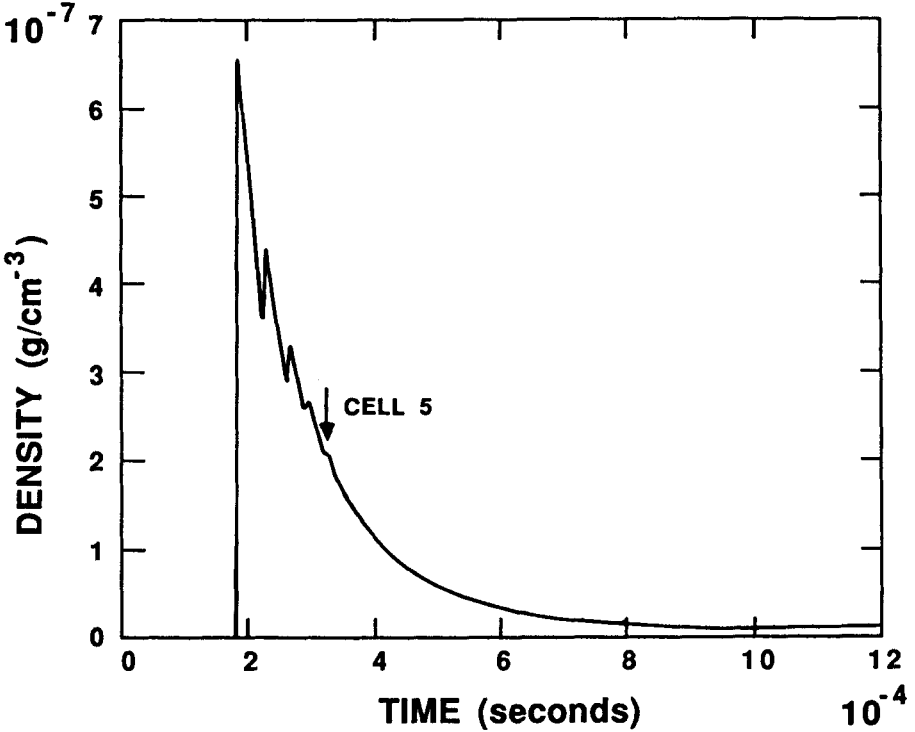

FIGURE 6

Computed total mass density of detonation product at the mass filter as a function of their arrival time after detonation. Cell 5 corresponds to the arrival time of the first NO_2. Dips in the curve are artifacts of using a finite cell size in the computation.

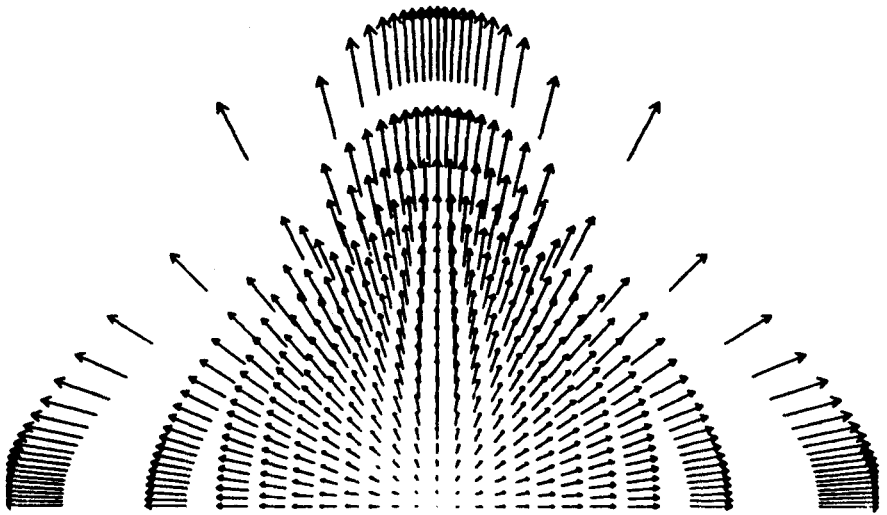

FIGURE 7

NORMAND C. BLAIS
ROY GREINER

Velocity field of the detonation products at 19.0 μs. The lengths of the arrows are proportional to the velocity, the long arrow corresponds to 6.6 km/s.

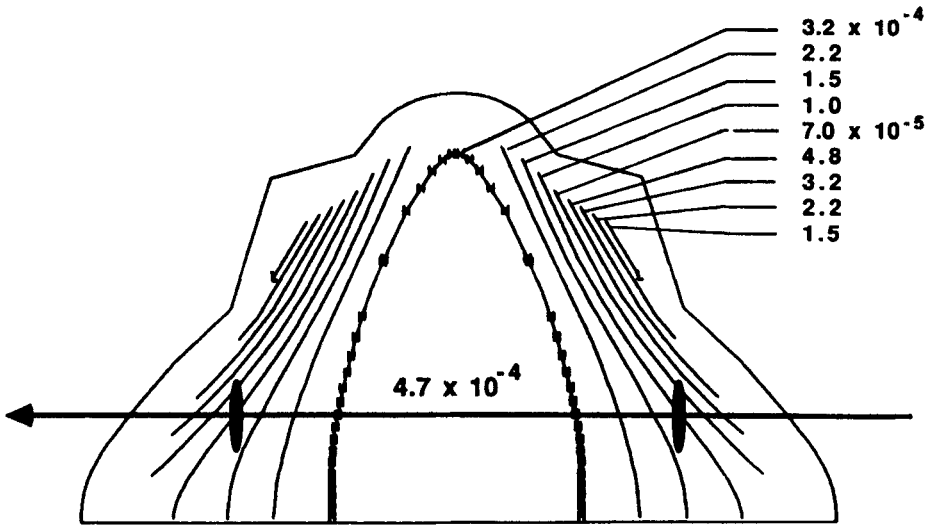

NORMAND C. BLAIS
ROY GREINER

FIGURE 8

Computed density profiles at 25 μs. Contours are in g/cm^3.

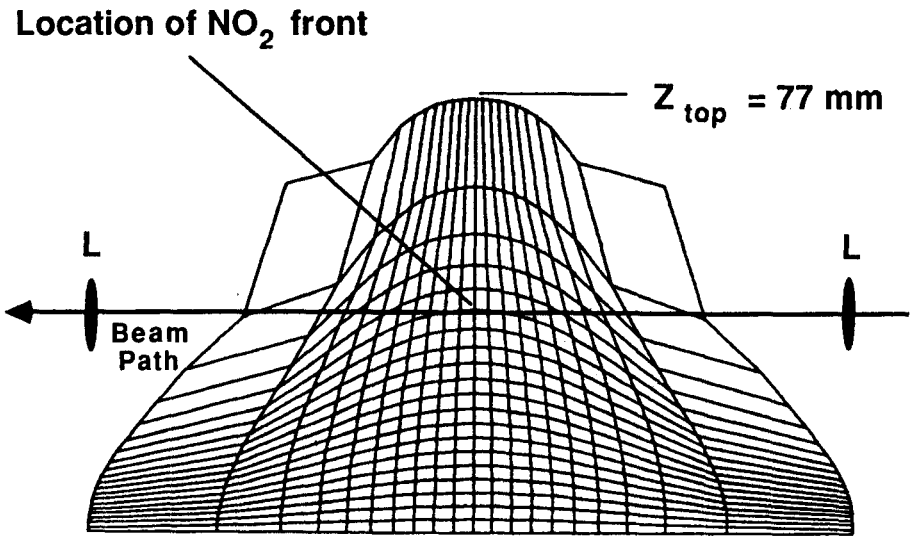

FIGURE 9

NORMAND C. BLAIS
ROY GREINER

Computational mesh at 11.5 μs, showing the optical path of the transmitted flashlamp light and the lenses (indicated by L). Each cell contains constant product mass during the expansion. The NO_2 front is at the rear of cell 5 (see Fig. 6).

gases, but this has no serious effect on the conclusions drawn here. The equations of state and the initial conditions are given in Table III.

TABLE III.
Calculational Inputs

Equation of State:

$P(dyne/cm^2) = 2.53 \times 10^{+10}\, d^{2.8} + 8.73 \times 10^{+9}\, d^{1.4}$; d in g/cm^3

Temperature: $T(K) = 2287\, d^{0.4}$

Initial Pressure: $1.245 \times 10^{+11}$ dyne/cm^2

Initial Density: 1.67 g/cm^3

Charge Shape: Right circular cylinder 1.2-cm diam x 0.355-cm high

Molecular Weight: 30 g/mol

The spectrum taken with 13-μs delay showed no absorption. The computed front of the NO_2 zone in the plume is found to be just arriving at the optical path at 12 μs (Fig. 9). At 25-μs delay, the peak of the NO_2 zone is past the optical path (Fig. 10), but within the optical path the NO_2 concentration is still about one-half of that of the peak. The calculations give an integrated concentration along this path of about 8×10^{-4} g/cm^2, with a temperature in the range 60-106 K (Fig. 11), whereas the observed spectrum compares with a calibration sample of 5×10^{-5} g/cm^2 at about 300 K. We explain the observation as follows: the absorption bands of NO_2 are known to become sharp as the molecule cools, which would tend to make the low-resolution spectrum weak, and evidently unobservable in our case. However, the calculations show that at this time the sides of the plume have collided with the lenses and other apparatus surfaces located on either side of the plume axis (Figs. 8, 9, and 11). As the plume collides with the lenses, it becomes compressed by momentum transfer (reshocking) and is heated to about 400 K. The quantity of gas reshocked is 4-7 $\times 10^{-5}$ g/cm^2, which compares with 5 $\times 10^{-5}$ g/cm^2 in the calibration samples run at 300 and 500 K (Fig. 5). We believe this is a plausible, if somewhat tentative explanation for the observed spectrum. It relies on the computed shape of the plume in a

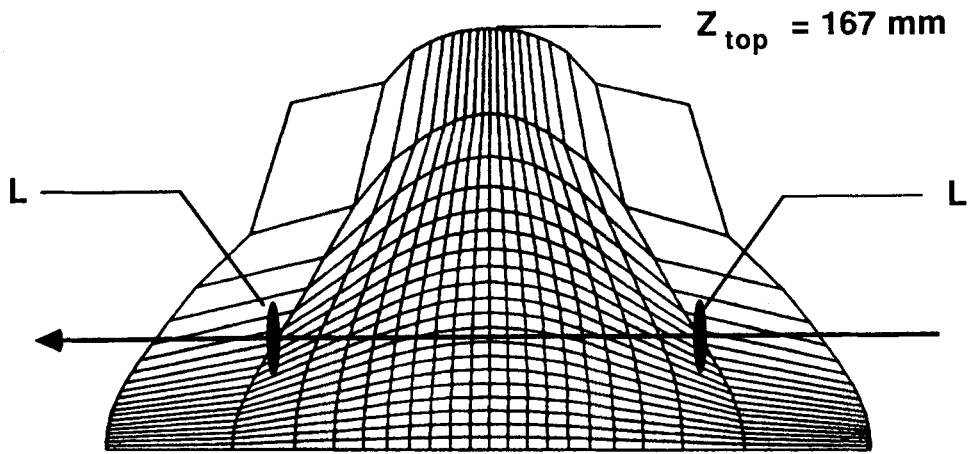

NORMAND C. BLAIS
ROY GREINER

FIGURE 10

Same as Fig. 9 except at a later time, 25 μs.

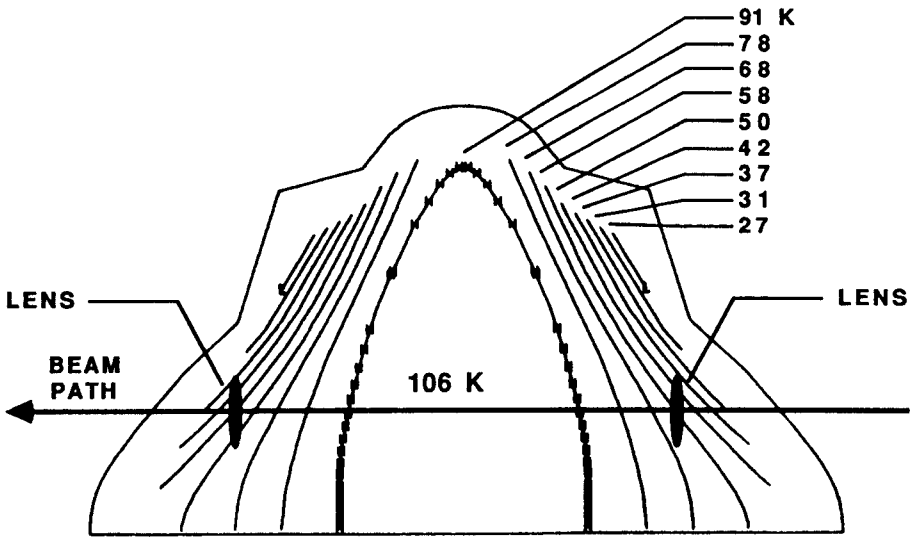

FIGURE 11

Computed temperature profile of the detonation products 15 μs after detonation.

NORMAND C. BLAIS
ROY GREINER

direction perpendicular to the z-axis, whereas our data give experimental support for the shape only along the z-axis.

CONCLUSION

We have determined the reaction products of shocked solid nitric oxide. From laboratory scale detonations, we find a simple mass spectrum consisting of N_2, O_2, N_2O and NO_2, and undetonated NO. We can account quantitatively for the intensities of the spectrum with a simple reaction scheme described by Eqs. (1), (2), and (3). These small scale detonations consumed about 65% of the NO charge in the viewing range of our detector, of which 29% lead to the products N_2 and O_2 in the detonation reaction, Eq. (1). About 50% of the O_2 product subsequently reacts with unreacted NO, as shown in Eq. (2), to form one-half of the observed NO_2.

The time-of-flight measurements of the product intensities indicate that the velocities of our products are determined by the hydrodynamic expansion phase of the process. The N_2 and O_2 originated near the surface of the nitric oxide charge and arrive earliest at the detector. The N_2O and NO_2 arrive measurably later, which suggest that they are formed in deeper regions of the product mix; where conditions of collision frequency and temperature are more favorable in their formation. The rate constant for reaction (2) is well known for gas phase conditions and room temperatures, and it has a negative temperature dependence. Therefore it seems reasonable that the product NO_2 would be more efficiently produced after the expansion has somewhat cooled the reagents, of which O_2 is itself a detonation product.

The absorption measurements confirm the importance of the hydrodynamic expansion in the final state distribution of products. The model we have developed indicates a rapid decrease in product temperature as the expansion occurs. However, where the computed density matches the condition at which we observe absorption, the calculated kinetic temperature is much lower than we estimate from

Fig. 5a. This may be because the absorption occurs in reshocked gas whose temperature was raised from the expansion temperature, or because the exoergic processes of secondary reactions were not properly taken into account in the model. We are inclined to think that reshocking is the cause, because the velocities of the absorbing molecules are lower than the measured values at the most probable density of gas. In any case, we want to point out that from these experiments we are able to present an identifiable spectrum whose internal and kinetic temperatures can be measured independently and correlated.

We point out that the reaction of Eq. (1), which occurs readily in condensed phase reactants, does not occur as a bimolecular reaction in the gas phase. Although N_2 and O_2 are reaction products of gas phase reactions of NO, they are ascribable to mechanism involving atom formation with subsequent atom-molecule reactions.[17] In highly shocked condensed phase experiments, especially in detonations, the conditions of temperature and density preclude these atom mechanisms. Insofar as there is any validity to using equilibrium constants determined at normal conditions, then at pressure of 10 GPa and a temperature of 3000 K an estimate of fractional dissociation of NO is 10^{-6}. Therefore the reaction leading to N_2 and O_2 must occur bimolecularly. Obtaining a detailed mechanism for this reaction promises to be very interesting.

ACKNOWLEDGMENTS

We wish to acknowledge the efforts of Wilbur Fernandez in the assembly and maintenance of the apparatus. We also received much help from Willard Hemsing and James Griffin in the Laboratory's Explosives Section, Group M-7, in designing and fabricating the detonators and cables. Peter O'Rourke assisted in and gave advice on the adaptation of the KIVA code to our problem and Jim Ritchie provided us with BKW calculations for the detonation products.

This paper was prepared under the auspices of the U.S. Department of Energy.

REFERENCES

1. John B. Ramsey and W. C. Chiles, Proceedings, Sixth Symposium (International) on Detonation, Coronado, California, 1976, p. 723.

2. J. Ribovich, J. Murphy, and R. J. Watson, "Detonation Studies with Nitrous Oxide, Nitric Oxide, Carbon Monoxide and Ethylene." J. Hazardous Mater. 1, 275 (1975).

3. W. C. Davis and W. C. Chiles, "Detonation Properties of Liquid Nitric Oxide," Preprints, Eighth Symposium (International) on Detonation, Albuquerque, NM 1985, p. 12.

4. Garry L. Schott, M. S. Shaw, and J. D. Johnson, "Shocked States From Initially Liquid Oxygen-Nitrogen Systems," J. Chem. Phys, 82, 4264 (1985).

5. N. C. Blais and J. J. Valentini, "Real-Time Analysis of PETN Detonation Products," Preprints, Eighth Symposium (International) on Detonation," V. 1, July 1985, p. 425.

6. CTI-Cryogenics Cryocooler. 15 watt capacity at 26 K with a 10 watt load at 77 K (first stage).

7. This was a nickel disk, 6-mm diam x 3-mm thick with 25-μm holes and open area of about 30%.

8. Cornu and Massot, "Compilation of Mass Spectral Data," 2nd edition, V. 1 (Heyden & Son 1979).

9. N. Blais, "Real-Time Analysis of HNS Detonation Products: Carbon Clusters, " J. of Energetic Materials 5, 57 (1987).

10. J. B. Anderson and J. B. Fenn, "Velocity Distributions in Molecular Beams from Nozzle Sources," Phys. Fluids 8, 780 (1965).

11. A molecular beam from a nozzle expansion of N_2O and NO_2 seeded to less than 5% into N_2 as a carrier was used to obtain the adjustment factors.

12. For gas phase conditions the reaction is termolecular with a rate constant $k = 3.3 \times 10^{-39} \exp(530/T)$ cm^6 $molecule^{-2}$ s^{-1}; see D. L. Baulch, R. A. Cox, R. F. Hampson, Jr., J. A. Kerr, J. Troe, and R. T. Watson, "Evaluated Kinetic and Photochemical Data for Atmospheric Chemistry: Supplement II,"J. Phys. Chem. Ref. Data, 13, 1259 (1984).

13 A. A. Amsden, J. D. Ramshaw, P. J. O'Rourke, and J. K. Dukowicz, "KIVA: A Computer Program for Two- and Three-Dimensional Fluid Flows with Chemical Reactions and Fuel Sprays," Report, LA–10245–MS, Los Alamos National Laboratory, Feb. 1985.

14. C. L. Mader, "Numerical Modeling of Detonations," University of California Press, Berkeley, 1979, Appendix E.

15. J. O. Hirschfelder, C. F. Curtis, and R. B. Bird, "Molecular Theory of Gases and Liquids," John Wiley and Sons, New York, 1954, p. 797.

16. J. P. Ritchie, private communication.

17. K. Thielen and P. Roth, "Resonance Absorption Measurements of N and O Atoms in High Temperature NO Dissociation and Formation Kinetics," Twentieth Symposium (International) on Combustion, The Combustion Institute, 1984, p. 685.